DOI: 10.1002/ejoc.201001073

Modeling and Spectroscopic Studies of Synthetic Diazabicyclo Analogs of the HIV-1 Inhibitor BMS-378806 and Evaluation of Their Antiviral Activity

Laura Legnani,[a] Diego Colombo,[b] Elena Cocchi,[c] Lucrezia Solano,[c] Stefania Villa,[c] Lucia Lopalco,[d] Valeria Asti,[d] Lorenzo Diomede,[d] Franca Marinone Albini,[a] and Lucio Toma*[a]

Keywords: Antiviral agents / Inhibitors / Molecular modeling / NMR spectroscopy

Three diazabicyclo analogs of BMS-378806, in which the axial methyl group present on its piperazine ring is replaced by a carbon bridge, were synthesized and tested, through a viral neutralization assay, on a panel of six pseudoviruses. The diazabicyclooctane and -nonane derivatives maintained a significant infectivity reduction power, whereas the diazabicycloheptane derivative was much less effective. A modeling study allowed to relate the antiviral activity to the conformational preferences of the compounds. Moreover, similarly to BMS-378806, theoretical calculations predict the existence of different conformational families corresponding to the possible arrangements at the two planar amido functions of the compounds. High-field ^{1}H NMR spectra confirm these results, as they show two distinct series of signals.

Introduction

AIDS is caused by the human immunodeficiency virus (HIV), a retrovirus with a RNA genome.[1] The UNAIDS Report 2009 estimated that 33.4 million people worldwide were living with HIV at the end of 2008.[2] In the absence of an effective preventive vaccine, anti-HIV drugs are urged to combat the expanding global epidemic.

Currently used anti-HIV therapy is a combination cocktail of inhibitors of HIV reverse transcriptase and protease; it allows an effective control of viral load and disease progression in HIV-infected individuals, prolonging the survival of AIDS patients. Nevertheless, the emergence of drug-resistant strains and the toxicity associated to the therapy have limited the efficacy of this regimen. Since the AIDS pandemic is one of the leading global public health threats, the discovery and development of new antiretroviral drugs with reduced toxicity, enhanced potency, different mechanisms of action, and reduced prevalence of adverse drug–drug interactions remain very high priorities. In particular, a promising area of investigation is the identification of agents that inhibit viral attachment and entry into host cells[3] in order to block HIV infection at the early stages.

The azaindole derivative BMS-378806 (**1**) (Scheme 1), discovered at Bristol–Myers Squibb,[4] has been shown to interfere with the HIV-1 entry process, inhibiting the interaction between the viral gp120 envelope glycoprotein and its cellular CD4 receptors[5] through a specific and competitive mechanism with a stoichiometry of approximately 1:1 and a binding affinity similar to that of soluble CD4. BMS-378806 retains activity against HIV strains resistant to protease and reverse transcriptase inhibitors and is active against viral strains with both the CCR5 and the CXCR4 coreceptors,[5] other very attractive targets for anti-HIV therapy. Its pharmacokinetic and pharmaceutical characteristics supported an oral formulation in man, but it was also being investigated in formulations for vaginal administration for the prevention of HIV-1 transmission when used in combination with other vaginal microbicides.[6]

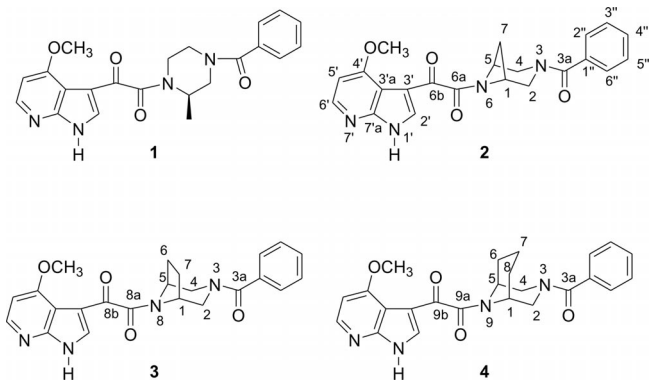

Scheme 1. Compounds **1**–**4**.

[a] Dipartimento di Chimica Organica, Università di Pavia,
Via Taramelli 10, 27100 Pavia, Italy
Fax: +39-0382-987323
E-mail: lucio.toma@unipv.it
[b] Dipartimento di Chimica, Biochimica e Biotecnologie per la Medicina, Università di Milano,
Via Saldini 50, 20133 Milano, Italy
[c] Dipartimento di Scienze Farmaceutiche "Pietro Pratesi", Università di Milano,
Via Mangiagalli 25, 20133 Milano, Italy
[d] Division of Immunology, Transplantation and Infectious Diseases, San Raffaele Scientific Institute,
Via Stamira D'Ancona 20, 20127 Milano, Italy

Supporting information for this article is available on the WWW under http://dx.doi.org/10.1002/ejoc.201001073.

We recently reported a full conformational evaluation of BMS-378806, which shows its high flexibility.[7] The located conformations were grouped into four families corresponding to the possible arrangements at the two planar amido functions and distinguishable in the NMR timescale. In fact, the high-field ^{1}H NMR spectrum of **1** shows four distinct series of signals easily attributable to each family, which thus supports the modeling results.

Starting from **1**, the design of structural analogs represents an important tool to obtaining new compounds possibly with even higher potency and/or better characteristics in their inhibitory activity against HIV-1.[8]

Some of us have a long-lasting experience in the synthesis of pharmacologically active compounds with a diazabicyclo moiety in their structure. So our interest has been directed to obtaining analogs of **1** in which the central piperazine ring is replaced by 3,6-diazabicyclo[3.1.1]heptane (**2**), 3,8-diazabicyclo[3.2.1]octane (**3**), or 3,9-diazabicyclo[3.3.1]-nonane (**4**) (Scheme 1). These compounds were prepared and, together with **1**, subjected to a viral neutralization assay[9] in order to investigate their pharmacological properties relative to the reference compound. Moreover, in an attempt to correlate the geometrical features and the conformational preferences of compounds **2**–**4** to their HIV-1 inhibitory activity, a modeling study was carried out with a computational approach, which was supported by a detailed NMR analysis of the new compounds.

Results and Discussion

Synthesis

All compounds were synthesized with a procedure similar to that already used for reference compound **1**,[4] starting from known[10] diazabicyclo precursors. Through the proper protection/deprotection steps, compounds **5** were converted into the benzoylated derivatives **9** and then into the target compounds (Schemes 2 and 3).

Two different approaches were used for the synthesis of the three required benzoylated diazabicycles **9**. The first, applied to the synthesis of **9b** and **9c** (Scheme 2), was based on the temporary protection of the secondary amino group of **5** with di-*tert*-butyl dicarbonate to allow debenzylation, achieved by catalytic hydrogenation with a heterogeneous Pd/C catalyst, and benzoylation of the unmasked amino group with benzoyl chloride in toluene. Acidic deprotection gave compounds **9b** and **9c**.

The same procedure to obtain **9a** presented many difficulties and too low yields because of the extreme instability of the diazabicyclo[3.1.1]heptane moiety, in particular during the cleavage reaction of the *tert*-butyloxycarbonyl group. Thus, the alternative approach described in Scheme 3 was applied in the preparation of **9a**. The benzyl derivative **5a** was treated with benzoyl chloride in toluene and then submitted to catalytic hydrogenation. The initially formed intermediate was not isolated, as it spontaneously rearranged into its isomer **9a** through an intramolecular transposition already observed for other diazabicyclo compounds.[10c]

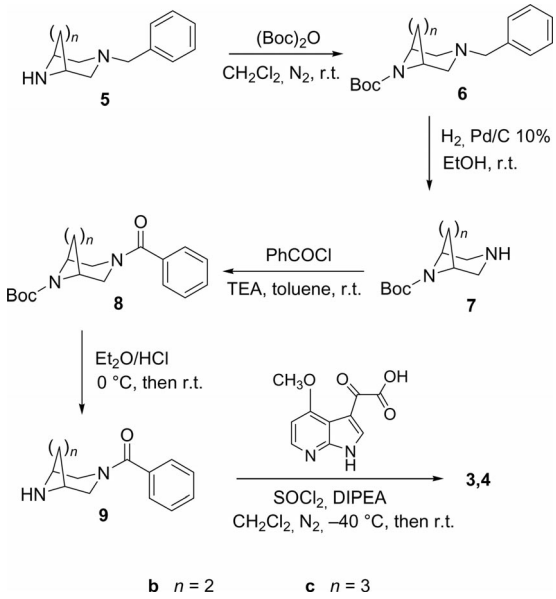

Scheme 2. Synthesis of compounds **3** and **4**.

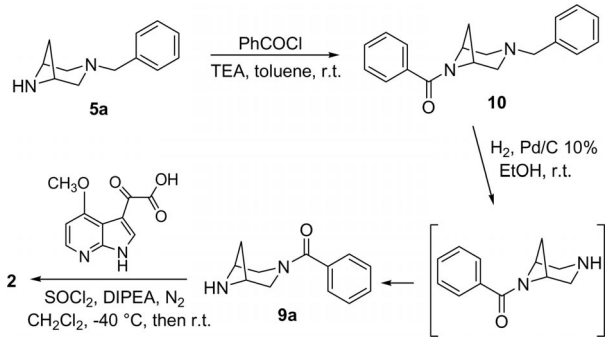

Scheme 3. Synthesis of compound **2**.

Finally, the target compounds **2**–**4** were obtained by reaction of the suitable benzoylated diazabicycles **9** with (4-methoxy-1*H*-pyrrolo[2,3-*b*]pyridine-3-yl)oxoacetic acid[11] (Schemes 2 and 3).

Biology

A standardized chemoluminescent assay[9] was performed to assess the infectivity reduction of all compounds under examination; in detail, BMS-378806 (**1**) and its three analogs **2**–**4** were tested. The infectivity reduction power was challenged on a panel of six pseudoviruses, including one laboratory strain SF162, four Clade B isolates QH0692, 6535, PVO, and AC10 and one Clade C primary virus ZM214. As a specificity negative control, an HIV-unrelated virus (SVA.MLV#922) was also included in the experiment to show that none of the compounds under assay affected its infectivity (data not shown).

Table 1 summarizes the data of infectivity reduction on the six pseudoviruses of the panel. Compound **1** efficiently neutralized all viruses tested with a mean IC_{50} of 0.01 μM; it also showed a mean IC_{90} and IC_{99} at low concentrations, 0.66 and 2.1 μM, respectively. Compounds **3** and **4** showed an infectivity reduction power lower than **1**; mean IC_{50}, IC_{90}, and IC_{99} values were 0.69, 29, and 71 μM, respectively, for **3** and 0.79, 29, and 70 μM, respectively, for **4**. On the contrary, analog **2** was much less effective than the other compounds as it showed no activity against QH0692 and reduced infectivity of the other viruses at 50% only with a mean IC_{50} of 145 μM. The positive control TriMab showed a range of IC_{50} from <0.25 to 9.1, of IC_{90} from 0.25 to >67, and of IC_{99} from 2.0 to >>67 μg/mL. As expected, in all these cases, including TriMab, the Clade C virus was less susceptible to neutralization than the Clade B viruses.

Table 1. HIV-1 infectivity reduction expressed as IC_{50}, IC_{90}, and IC_{99} [μM] by BMS-378806 (**1**) and its analogs **2**–**4** in a TZM-bl cell assay with a panel of six different viruses.

Viruses	Clade	IC_x[a]	**1**	**2**	**3**	**4**	TriMab[b]
SF162	Laboratory Strain B	IC_{50}	0.002	140	0.36	0.39	<0.25
		IC_{90}	0.49	>250	32	42	0.25
		IC_{99}	3.2	>>250	88	120	2.0
QH0692	Primary B	IC_{50}	0.02	>>250	1.2	1.9	<0.25
		IC_{90}	2.1	>>250	56	57	3.0
		IC_{99}	5.2	>>250	133	124	10
6535	Primary B	IC_{50}	<0.002	70	0.02	0.02	0.08
		IC_{90}	0.005	>250	1.4	6.7	8.3
		IC_{99}	0.10	>>250	4.0	22	24
PVO	Primary B	IC_{50}	0.002	175	0.24	0.51	<0.25
		IC_{90}	0.22	>250	9.4	18	0.53
		IC_{99}	0.42	>>250	22	41	4.7
AC10	Primary B	IC_{50}	0.02	185	1.1	1.1	0.46
		IC_{90}	0.69	>250	18	13	21
		IC_{99}	1.4	>>250	33	22	50
ZM214	Primary C	IC_{50}	0.005	153	1.1	0.83	9.1
		IC_{90}	0.49	>250	59	38	>67
		IC_{99}	2.5	>>250	144	89	>>67

[a] IC_{50}, IC_{90}, and IC_{99} stand for the compound concentration leading to 50, 90, and 99% of infectivity reduction, respectively. [b] Positive control [μg/mL].

Modeling

Theoretical calculations were performed within the DFT approach at the B3LYP level with the 6-31G(d) basis set.[12] Solvent effects were also considered through single-point calculations on the gas-phase optimized geometries, by using a self-consistent reaction field (SCRF) method, based on the polarizable continuum model (PCM),[13] and by choosing water as the solvent. However, the solvent does not significantly influence the results so that, in the following discussion, it will not be considered.

As already found for **1**,[7] we also expected for **2**–**4** the presence of four conformational families, which correspond to the four different combinations of arrangements of the C–N bonds of the two amido functions and which differ in the torsional angles τ_1 and τ_2. Additional degrees of conformational freedom arise because of the presence of the diazabicyclo system and the substituents on the two piperazine nitrogen atoms. The mobility of the former system may derive from the chair/boat interconversion of the piperazine ring and, in the case of **4**, of that of the piperidine ring. The arrangement of the 1,2-dioxo system, the orientation of the azaindole moiety, the orientation of the methoxy group, and that of the benzoyl phenyl group allow the conformational flexibility of the substituents. All the corresponding starting geometries were prepared and optimized. Tenths of minimum energy conformers were located and grouped into four families (**A**–**D**). The symmetry of the diazabicyclo systems makes the members of the **A** family mirror images of the members of the **D** family and the same relationship holds true between the members of the **B** and **C** families. A lower number of conformers were located for the diazabicycloheptane derivative **2** as, in this case, the 1,2-dioxo system showed only one minimum instead of the two arrangements found for all the other compounds. A larger number of conformers were located for the diazabicyclononane analog **4** because of the greater conformational freedom of the bicyclic moiety. In Table 2, the gas-phase energies of the most-stable member of each family for the three analogs and the percentage contribution of each family to the overall population are reported, together with the torsional angles defining the orientation of the amido functions. In Figure 1, the corresponding three-dimensional plots for the **A** and **B** families are reported.

Table 2. Relative energies [kcal/mol], equilibrium percentages at 248 K, and significant torsional angles[a] [°] of significant conformations of compounds **2**–**4**.

	E_{rel}	%	τ_1	τ_2
2A	0.06	23.4	24	176
2B	0.00	26.6	–171	176
2C	0.00	26.6	23	16
2D	0.06	23.4	–171	15
3A	0.10	22.7	6	172
3B	0.00	27.3	–172	173
3C	0.00	27.3	6	27
3D	0.10	22.7	–173	28
4A	0.07	25.2	–4	169
4B	0.00	24.8	–170	169
4C	0.00	24.8	–4	22
4D	0.07	25.2	–171	22

[a] τ_1: C1–N*x*–C*x*a–C*x*b; (*x* = 6 for **2**, *x* = 8 for **3**, *x* = 9 for **4**); τ_2: C2–N3–C3a–C1′′.

In order to put in better evidence analogies and differences among the conformations of the various compounds and to compare them with reference compound **1**,[7] we superimposed, through the rms fitting of the six atoms of the piperazine ring, the conformations of **1**–**4** holding the same label. As examples, in Figure 2, the superimpositions of the **A** and **B** geometries are reported.

It can be seen that the orientation of the azaindole group is quite different in the four compounds, as well as that of the benzoyl phenyl group. With respect to **1**, a progressive deviation of the two aromatic systems towards a direction

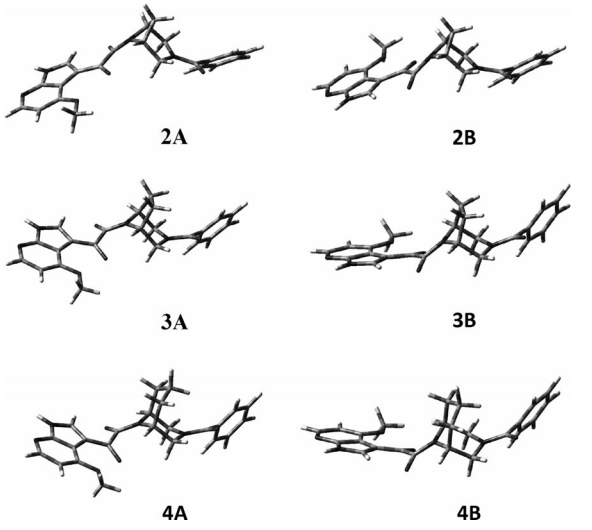

Figure 1. Three-dimensional plots of the most-stable members of the **A** and **B** conformational families of compounds **2**–**4**.

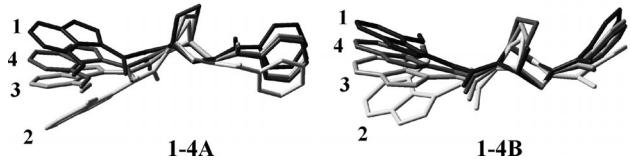

Figure 2. Superimpositions of the most-stable members of the **A** and **B** conformational families of compounds **1**–**4**.

opposite to the aliphatic bridge is observed, more pronounced for the azaindole group, especially in the case of **2**, where the deviation is very significant.

Table 3. B3LYP/6-31G(d) GIAO calculated ^{1}H NMR chemical shift (δ, in ppm relative to TMS) for compounds **2**–**4**, based on the geometries optimized at the same level. The experimental values from the spectra recorded in CD_3OD are given for comparison.

		A/D families		**B/C** families	
Compound	H	$\delta_{calcd.}$	$\delta_{exp.}$	$\delta_{calcd.}$	$\delta_{exp.}$
2[a]	1	4.85	4.75	4.28	4.75
	2ax	4.00	4.11	3.73	4.11
	2eq	4.54	4.19	4.45	4.11
	4ax	4.23	4.07	4.54	4.01
	4eq	3.28	3.71	3.44	3.73
	5	4.12	4.56	4.63	4.56
3	1	4.43	4.30	4.60	4.89
	2ax	3.47	3.26	2.94	3.22
	2eq	4.56	4.59	4.55	4.70
	4ax	3.47	3.63	4.03	3.67
	4eq	3.57	3.64	3.61	3.56
	5	4.44	4.69	4.22	4.10
4	1	4.12	4.00	4.64	4.83
	2ax	3.14	3.21	2.96	3.33
	2eq	4.67	4.75	4.72	4.89
	4ax	3.44	3.70	3.73	3.59
	4eq	3.76	3.90	3.72	3.78
	5	4.48	4.64	3.96	3.81

[a] In the case of compound **2**, the assignment of the resonances of the **A/D** and **B/C** families may be interchanged.

At last, we computed the ^{1}H NMR chemical shifts for each populated conformation of compounds **2**–**4** by using GIAO NMR calculations[14] at the same level already used for the optimizations.[15] The obtained values were weighted, averaged, separately for the conformations of every family, on the basis of the population percentages. The chemical shift values for the hydrogen atoms of the piperazine rings are reported in Table 3, together with the corresponding experimental data (see below).

NMR Spectroscopy

High-field ^{1}H NMR spectra in [D_4]methanol were recorded at 248 K because compounds **3** and **4** show broad signals as a result of coalescence at 298 K. On the contrary, the proton resonances have a good shape and resolution at the selected temperature. As expected, all the spectra show two distinct series of signals, which correspond to the two couples of conformational families **A/D** and **B/C** predicted by the calculations. As convenient entry points for the resonances assignment, the protons linked to the tertiary bridgehead carbon atoms of the bicyclic systems, easily determined by HSQC experiments, were used. The spectra could also be divided into three zones on the basis of the effect of the amidic carbonyl groups on the chemical shifts of the diazabicycle protons:[7] (a) from 5.00 to 4.50 ppm (equatorial piperazine protons, which are strongly influenced by the deshielding effect of amidic carbonyls), (b) from 4.35 to 3.00 ppm (the other piperazine protons) and (c) from 3.00 to 1.40 (the bridge protons, lowest deshielding effect). In this way, it was possible to assign (Table 3), through COSY and HSQC experiments, 2-Heq and 5-H (4.59 and 4.69 ppm, respectively, **A/D** families) and 2-Heq and 1-H (4.70 and 4.89 ppm, respectively, **B/C** families) for compound **3** and the corresponding resonances (4.75, 4.64, 4.89, and 4.83 ppm) for compound **4**. These signals from 5.00 to 4.50 ppm, deshielded by the carbonyl groups, represent the key points for the conformational assignment. The remaining 2-H as well as the 4-H resonances were then assigned. In particular, COSY cross peaks, as a result of the long-range couplings between the equatorial 2-H (4.59 and 4.70 ppm for compound **3** and 4.75 and 4.89 ppm for compound **4**) and 4-H, allow to assign the axial/equatorial geminal 4-H protons. Finally, through a careful study of the 2D spectra, the protons of the di- and trimethylene bridges of **3** and **4** can also be assigned (see Supporting Information).

Differently, compound **2** shows two signals at δ = 4.75 and 4.56 ppm in its spectrum, which account for the four bridgehead 1-H and 5-H protons (clearly detected by HSQC). The coupling of these protons with the two characteristic high-field 7-H bridge protons at δ = 2.86 ppm (9.1 Hz) and 1.80/1.81 ppm (weak COSY cross peak) and with the other two couples of methylene protons (2-H and 4-H) confirms the assignments. Also, in this case, the assignment of the axial/equatorial orientation to the geminal protons was possible because of the long-range couplings between 2-Heq and 4-Heq. Unfortunately, the overlapping

of all the 1-H signals as well as the 5-H signals did not allow the assignment of the resonances to the corresponding conformational series.

The signals for the azaindole protons of all the studied compounds could be also determined under these experimental conditions – they appear as well-separated sharp signals for the two conformational series, that, however, could not be assigned (see Supporting Information): two singlets for 2-H′ (8.26–8.40 ppm), two doublets (J = 5.8 Hz) for 6-H′ (8.22–8.27 ppm), two doublets (J = 5.8 Hz) for 5-H′ (6.90–6.96 ppm). The two well-resolved methoxy singlets at 3.99–4.04 ppm and the multiplet at 7.38–7.56 ppm, which account for the five benzoyl protons, completed the description of the ^{1}H NMR spectra of compounds **2**–**4**.

Finally, for all the compounds a relative ratio close to 1:1 of the **A/D** and **B/C** conformational families was detected by careful integration of some well-resolved ^{1}H signals. These data confirm those predicted by calculations (Table 2). In particular, a 51:49 ratio for compound **4** was deduced from the 5**A**-H/1**B**-H and 2eq**A**-H/2eq**B**-H resonances (Table 3). The same 51:49 ratio was observed for **3** (2eq**A**-H/1**B**-H).

Conclusions

Three structural analogs of BMS-378806 **1**, in which the axial methyl group present on its piperazine ring is replaced by a methylene, dimethylene, or trimethylene bridge, were synthesized and their infectivity reduction power determined relative to the reference compound, through a viral neutralization assay on a panel of six pseudoviruses.

All compounds under assay neutralized the viral strains, although they reduced the virus infectivity to different extents. Diazabicyclooctane **3** and diazabicyclononane **4** maintained a significant infectivity reduction power, whereas diazabicycloheptane **2** was much less effective.

Theoretical calculations show a very high degree of molecular flexibility for the analogs **2**–**4**. The same four conformational families, already found in **1**, corresponding to the possible arrangements at the two planar amido functions, were located. The high-field ^{1}H NMR spectra of the compounds confirm these results and show two distinct series of signals attributed to the **A/D** and **B/C** couples of the conformational families predicted by the calculations.

A comparison of the biological data with the modeling results suggests that the conformational preferences of this class of small molecules are determinant for their antiviral activity. In fact, the modeling studies evidence a progressive deviation of the azaindole and benzoyl groups towards a direction opposite to the aliphatic bridge in compounds **2**–**4** with respect to those in **1**, more pronounced for the azaindole group, especially in the case of **2**. The antiviral activity of **3** and **4** suggests that a small deviation of the azaindole system with respect to the position occupied in **1** is tolerated, while a larger deviation in the same direction, as in **2**, causes an almost complete loss of activity. The steric hindrance of the aliphatic bridge present in **2**–**4** does not seem to exert a major influence on the biological properties, as compound **4**, which contains a larger carbon bridge, shows antiviral activity almost comparable to that of **3** and much better than that of **2**, although the latter compound is, in size, most similar to **1**.

Experimental Section

General: All materials were purchased from Sigma–Aldrich and were used without any further purification. All reactions involving air-sensitive reagents were performed under a nitrogen atmosphere. Reactions were monitored by thin layer chromatography (TLC) on an aluminum-backed Silica Gel 60 plates (0.2 mm, Merck). The compounds were purified by flash chromatography by using Merck Silica Gel 60 (70–230 mesh). Melting points were determined in open capillary tubes on a Büchi Melting Point B-540 apparatus. ^{1}H NMR spectra of intermediates were acquired at 298 K on a Varian 300 MHz Oxford instrument. Mass spectrometry was performed on a Thermo Electron TRACE DSQTM spectrometer through the rapid heating filament direct-exposure probe (DEP) insertion mode. The mass spectrometric analyses were performed in chemical ionization (CI–MS) by using methane as reactant gas at an electron energy of 70 eV with a source temperature of 200 °C.

6-Benzoyl-3-benzyl-3,6-diazabicyclo[3.1.1]heptane (10): To a solution of 3-benzyl-3,6-diazabicyclo[3.1.1]heptane (**5a**)[10a] (1.10 g, 5.84 mmol) in toluene (12 mL) were added triethylamine (5.84 mmol) and benzoyl chloride (5.84 mmol). The reaction mixture was stirred at room temperature overnight. The salts were filtered off, and the solvent was evaporated to give the crude product. The residue was purified by flash chromatography by eluting with petroleum ether (PE)/EtOAc (1:1) to give compound **10** (1.11 g, 65%): R_f = 0.26 (PE/EtOAc, 1:1). ^{1}H NMR (300 MHz, $CDCl_3$): δ = 2.00–2.10 (m, 1 H, 7a-H), 2.55–2.70 (m, 2 H, 7b-H and 4a-H), 2.80–3.00 (m, 2 H, 2a-H and 4b-H), 3.30–3.40 (m, 1 H, 2b-H), 3.65–3.75 (m, 2 H, CH_2Ph), 4.35–4.45 (m, 1 H, 5-H), 4.50–4.60 (m, 1 H, 1-H), 7.20–7.65 (m, 10 H, arom.) ppm. $C_{19}H_{20}N_2O$ (292.37): calcd. C 78.05, H 6.89, N 9.58; found C 78.26, H 6.79, N 9.62.

3-Benzoyl-3,6-diazabicyclo[3.1.1]heptane (9a): A solution of 6-benzoyl-3-benzyl-3,6-diazabicyclo[3.1.1]heptane (**10**) (0.70 g, 2.39 mmol) in EtOH (40 mL) was hydrogenated at 3 atm and 60 °C in the presence of 10% Pd–C (10:1 w/w) for 72 h. The catalyst was filtered off through Celite, and the solvent was evaporated. The residue was purified by flash chromatography by eluting with EtOAc/MeOH (7:3) to give compound **9a** as a yellow solid (0.26 g, 53%): R_f = 0.10 (EtOAc/MeOH, 7:3). ^{1}H NMR (300 MHz, $CDCl_3$): δ = 1.50–1.60 (m, 1 H, 7a-H), 1.75–1.85 (m, 1 H, NH), 2.65–2.75 (m, 1 H, 7b-H), 3.55–3.65 (m, 3 H, 1-H, 4a-H, 5-H), 3.75–3.90 (m, 2 H, 2a-H and 4b-H), 4.00–4.10 (m, 1 H, 2b-H), 7.35–7.45 (m, 5 H, arom.) ppm. $C_{12}H_{14}N_2O$ (202.25): calcd. C 71.26, H 6.98, N 13.85; found C 71.12, H 7.09, N 13.99.

1-(3-Benzoyl-3,6-diazabicyclo[3.1.1]hept-6-yl)-2-(4-methoxy-1*H*-pyrrolo[2,3-*b*]pyridin-3-yl)ethane-1,2-dione (2): To a solution of (4-methoxy-1*H*-pyrrolo[2,3-*b*]pyridin-3-yl)oxoacetic acid (0.454 mmol) in dry CH_2Cl_2 (6 mL) under a nitrogen atmosphere was added $SOCl_2$ (0.454 mmol), and the mixture was heated to reflux for 1 h. The reaction was cooled to –40 °C, and a solution of compound **9a** (92 mg, 0.455 mmol) and DIPEA (1.82 mmol) in CH_2Cl_2 (4 mL) was added very slowly. The mixture was warmed to room temperature and stirred overnight. The reaction was quenched with 17% NaCl, and the mixture was extracted with CH_2Cl_2. The or-

ganic layers were dried with Na_2SO_4, and the solvents evaporated under vacuum. The residue was purified by flash chromatography by eluting with EtOAc/MeOH (10:1). The product was washed with Et_2O at room temperature and filtered to give compound **2** as a white solid (46 mg, 25%): R_f = 0.13 (EtOAc/MeOH, 10:1). M.p. 171–173 °C. CI-MS: *m*/*z* = 405.2 $[M + H]^+$. $C_{22}H_{20}N_4O_4$ (404.42): calcd. C 65.34, H 4.98, N 13.85; found C 65.49, H 5.12, N 13.73.

3-Benzoyl-8-*tert*-butyloxycarbonyl-3,8-diazabicyclo[3.2.1]octane (8b): With the same procedure already described in the conversion of **5a** to **10**, starting from compound **7b**[10b] (1.04 g, 4.90 mmol), compound **8b** was obtained as a brown oil (1.44 g, 93%): R_f = 0.13 (PE/EtOAc, 8:2). ^1H NMR (300 MHz, $CDCl_3$): δ = 1.45 (s, 9 H, CMe_3), 1.70–1.95 (m, 4 H, 6-H_2 and 7-H_2), 2.95–3.10 (m, 1 H, 2a-H), 3.30–3.40 (m, 2 H, 4-H_2), 4.00–4.55 (m, 3 H, 1-H, 2b-H, and 5-H), 7.25–7.40 (m, 5 H, arom.) ppm. $C_{18}H_{24}N_2O_3$ (316.39): calcd. C 68.33, H 7.65, N 8.85; found C 68.57, H 7.82, N 8.70.

3-Benzoyl-3,8-diazabicyclo[3.2.1]octane (9b): To a solution of compound **8b** (0.75 g, 2.37 mmol) in Et_2O (20 mL) at 0 °C was added a solution of Et_2O·HCl (40 mL). The reaction mixture was warmed to room temperature and stirred for 2.5 d. A solution of 6 M NaOH was added until pH = 10, and the mixture was extracted with Et_2O. The organic layers were dried with Na_2SO_4, and the solvents evaporated under vacuum to give **9b** (0.49 g, 95%): R_f = 0.67 (CH_2Cl_2/MeOH, 8:2). ^1H NMR (300 MHz, $CDCl_3$): δ = 1.65–1.95 (m, 5 H, 6-H_2, 7-H_2, and NH), 2.95–3.10 (m, 1 H, 2a-H), 3.30–3.70 (m, 4 H, 1-H, 4-H_2, 5-H), 4.40–4.55 (m, 1 H, 2b-H), 7.25–7.40 (m, 5 H, arom.) ppm. $C_{13}H_{16}N_2O$ (216.28): calcd. C 72.19, H 7.46, N 12.95; found C 71.98, H 7.57, N 13.04.

1-(3-Benzoyl-3,8-diaza-bicyclo[3.2.1]oct-8-yl)-2-(4-methoxy-1*H*-pyrrolo[2,3-*b*]pyridin-3-yl)ethane-1,2-dione (3): With the same procedure already described in the conversion of **9a** to **2**, starting from compound **9b** (105 mg, 0.486 mmol), compound **3** was obtained as a yellow solid (53 mg, 26%): R_f = 0.22 (EtOAc/MeOH, 10:1). M.p. 247–250 °C (dec.). CI-MS: *m*/*z* = 419.2 $[M + H]^+$. R_f = 0.67 (CH_2Cl_2/MeOH, 8:2). $C_{23}H_{22}N_4O_4$ (418.45): calcd. C 66.02, H 5.30, N 13.39; found C 66.23, H 5.45, N 13.11.

3-Benzyl-9-*tert*-butyloxycarbonyl-3,9-diazabicyclo[3.3.1]nonane (6c): To a solution of 3-benzyl-3,9-diazabicyclo[3.3.1]nonane **5c**[10c] (1.08 g, 4.97 mmol) in dry CH_2Cl_2 (10 mL) under a nitrogen atmosphere was added di-*tert*-butyl dicarbonate (4.97 mmol). The reaction mixture was stirred at room temperature overnight. The mixture was evaporated, and the product was purified by flash chromatography by eluting with cyclohexane/EtOAc (98:2) to give compound **6c** as a yellow oil (1.51 g, 96%): R_f = 0.40 (cyclohexane/EtOAc, 98:2). ^1H NMR (300 MHz, $CDCl_3$): δ = 1.45 (s, 9 H, CMe_3), 1.60–1.90 (m, 5 H, 6-H_2, 7a-H, 8-H_2), 2.20–2.35 (m, 2 H, 2a-H, and 7b-H), 2.75–2.90 (m, 3 H, 2b-H and 4-H_2), 3.40 (s, 2 H, CH_2Ph), 4.05 (m, 1 H, 5-H), 4.15 (m, 1 H, 1-H), 7.20–7.40 (m, 5 H, arom.) ppm. $C_{19}H_{28}N_2O_2$ (316.44): calcd. C 72.12, H 8.92, N 8.85; found C 72.39, H 8.69, N 8.63.

9-*tert*-Butyloxycarbonyl-3,9-diazabicyclo[3.3.1]nonane (7c): A solution of 3-benzyl-9-*tert*-butyloxycarbonyl-3,9-diazabicyclo[3.3.1]-nonane **6c** (1.40 g, 4.42 mmol) in EtOH (30 mL) was hydrogenated overnight at 3 atm and at room temperature in the presence of 10% Pd-C (10:1 w/w). The catalyst was filtered off through Celite, and the solvent was evaporated to give **7c** as a yellow oil (0.99 g, 99%): R_f = 0.48 (CH_2Cl_2/MeOH, 9:1). ^1H NMR (300 MHz, $CDCl_3$): δ = 1.45 (s, 9 H, CMe_3), 1.60–1.90 (m, 6 H, 6-H_2, 7a-H, 8-H_2, NH), 2.35–2.50 (m, 1 H, 7b-H), 2.85–3.15 (m, 4 H, 2-H_2 and 4-H_2), 3.95 (m, 1 H, 5-H), 4.10 (m, 1 H, 1-H) ppm. $C_{12}H_{22}N_2O_2$ (226.32): calcd. C 63.68, H 9.80, N 12.38; found C 63.75, H 10.01, N 12.22.

3-Benzoyl-9-*tert*-butyloxycarbonyl-3,9-diazabicyclo[3.3.1]nonane (8c): With the same procedure already described in the conversion of **7b** to **8b**, starting from compound **7c** (0.98 g, 4.33 mmol), compound **8c** was obtained as a white solid (1.00 g, 70%): R_f = 0.15 (PE/EtOAc, 8:2). ^1H NMR (300 MHz, $CDCl_3$): δ = 1.45 (s, 9 H, CMe_3), 1.50–1.95 (m, 5 H, 6-H_2, 7a-H, and 8-H_2), 2.05–2.20 (m, 1 H, 7b-H), 3.05–3.20 (m, 1 H, 2a-H), 3.35–3.45 (m, 1 H, 4a-H), 3.65–3.75 (m, 1 H, 4b-H), 4.00–4.40 (m, 2 H, 1-H and 5-H), 4.75–4.80 (m, 1 H, 2b-H), 7.35–7.45 (m, 5 H, arom.) ppm. $C_{19}H_{26}N_2O_3$ (330.42): calcd. C 69.06, H 7.93, N 8.48; found C 69.19, H 7.78, N 8.60.

3-Benzoyl-3,9-diazabicyclo[3.3.1]nonane (9c): With the same procedure already described in the conversion of **8b** to **9b**, starting from compound **8c** (0.89 g, 2.69 mmol), compound **9c** was obtained (0.56 g, 90%): R_f = 0.43 (CH_2Cl_2/MeOH, 9:1). ^1H NMR (300 MHz, $CDCl_3$): δ = 1.60–1.95 (m, 5 H, 6-H_2, 7a-H, and 8-H_2), 2.05–2.25 (m, 2 H, 7b-H and NH), 2.90–3.00 (m, 1 H, 5-H), 3.15–3.25 (m, 2 H, 1-H and 2a-H), 3.40–3.50 (m, 1 H, 4a-H), 3.65–3.75 (m, 1 H, 4b-H), 4.65–4.75 (m, 1 H, 2b-H), 7.30–7.45 (m, 5 H, arom.) ppm. $C_{14}H_{18}N_2O$ (230.31): calcd. C 73.01, H 7.88, N 12.16; found C 73.24, H 7.71, N 12.23.

1-(3-Benzoyl-3,9-diaza-bicyclo[3.3.1]non-9-yl)-2-(4-methoxy-1*H*-pyrrolo[2,3-*b*]pyridin-3-yl)ethane-1,2-dione (4): With the same procedure already described in the conversion of **9a** to **2**, starting from compound **9c** (102 mg, 0.443 mmol), compound **4** was obtained as a yellow solid (39 mg, 20%): R_f = 0.86 (EtOAc/MeOH, 10:1). M.p. 234–236 °C (dec.). CI-MS: *m*/*z* = 433.3 $[M + H]^+$. $C_{24}H_{24}N_4O_4$ (432.47): calcd. C 66.65, H 5.59, N 12.96; found C 66.79, H 5.70, N 12.83.

Viral Infectivity Reduction Assay: Infectivity reduction was measured as a reduction in Luc reporter gene expression after a single round of virus infection in TZM-bl cells with env-pseudotyped viruses.[9] Virus panel of HIV-related pseudoviruses included one laboratory strain SF162 (Clade B), four from primary infected Subtype B subjects such as QH0692, 6535, PVO, and AC10 isolates (all strains were CCR5-tropic), and one primary infected Subtype C virus, ZM214 (CCR5-tropic). In order to demonstrate the specificity of HIV neutralization, an HIV-unrelated virus (VSV-G virus, strain SVA.MLV#922) was also included. Briefly, 200 TCID50 of pseudoviruses in 50 µL culture media was incubated with 100 µL of serially diluted compounds (from 250 to 0.002 µM) or TriMab (containing 2G12, IgG1b12, and 2F5, 50:50:50 µg/mL), by using D-MEM with 10% foetal bovine serum in a 96-well plate for 1 h at 37 °C. A 100-µL solution of TZM-bl cells (1×10^4 cells/well) containing 15 µg/mL DEAE dextran was added; the cultures were then incubated at 37 °C in 5% CO_2/95% air for 48 h. Infection was monitored by evaluating the luciferase activity. Infectivity reduction was calculated as IC_{50}, IC_{90}, and IC_{99}, the compound concentration at which relative luminescence units (RLU) were reduced by 50%, 90% and 99% respectively, relative to virus control wells (wells with no inhibitor) after subtraction of background RLU in the cell control wells (wells without virus infection).

Computational Methods: A systematic search of the conformational space of compounds **2**–**4** was performed by using the Gaussian 03 program package[16] through optimizations in the gas phase at the B3LYP/6-31G(d) level.[12] First, a starting geometry presenting the **A** arrangement at the amido functions was optimized. Then, the energy profiles for rotation around the single bonds of the substituents on the nitrogen atoms were determined with a step size of 30°, and ring inversion of the piperazine and piperidine rings was performed. All the combinations of the observed minima were used to generate starting geometries optimized as above. The procedure

was similarly repeated for the **B** arrangement. Vibrational frequencies were computed at the same level of theory to verify that the optimized structures were minima. The population percentages were calculated through the Boltzmann equation at 248 K. GIAO NMR calculations[14] were carried out at the B3LYP/6-31G(d) level.

NMR Spectroscopy: NMR spectra of compounds **2**–**4** were recorded with a Bruker AVANCE-500 spectrometer operating at 500.13 MHz for ^{1}H or at 125.76 MHz for ^{13}C NMR spectra by using a 5-mm z-PFG (pulsed field gradient) broadband reverse probe at different temperatures obtained through a Bruker BVT 3000 digital temperature control unit connected to a liquid nitrogen evaporator system. Chemical shifts (δ) are reported in ppm and are relative to residual methanol signals (δ =3.30 ppm) or 47.0 ppm (central line) for CD_3OD ^{13}C NMR spectra, and scalar coupling constants are reported in Hz. The data were collected and processed by XWIN-NMR software (Bruker) running on a PC with Microsoft Windows XP. Compounds **2**–**4** (4–8 mg) were dissolved in CD_3OD (0.6 mL) and put in 5-mm NMR tubes. The signal assignment was given by a combination of 1D and 2D (COSY and HSQC) experiments, by using standard Bruker pulse programs. The ^{1}H-^{1}H and ^{13}C-^{1}H bond correlations were confirmed by COSY and HSQC experiment by using Z-PFGs. The pulse widths were 8.00 μs (90°) for ^{1}H and 13.6 μs (90°) for ^{13}C. Typically, 32 K data points were collected for one-dimensional spectra. Spectral widths were 11.45 ppm (5733 Hz) for ^{1}H NMR (digital resolution: 0.17 Hz per point) and 259.84 ppm (32680 Hz) for ^{13}C NMR (digital resolution: 1.0 Hz per point), 1.5 Hz line broadening. 2D experiment parameters were as follows. For ^{1}H-^{1}H correlations: relaxation delay 2.0 s, data matrix 1 K × 1 K (512 experiments to 1 K zero filling in F_1, 1 K in F_2), 2 transients in each experiment for COSY, spectral width 8.01 ppm (4006.41 Hz). For ^{13}C-^{1}H correlations (HSQC): relaxation delay 2.5 s, data matrix 1K × 1K (512 experiments to 1 K zero filling in F_1, 1K in F_2), 8 transients in each experiment, spectral width 8.0 ppm (4001 Hz) in the proton domain and 200.0 ppm (25155 Hz) in the carbon domain. A sine-bell weighting was applied to each dimension. All 2D spectra were processed with the Bruker software package.

Supporting Information (see footnote on the first page of this article): Complete ^{1}H and ^{13}C NMR spectroscopic data of compounds **2**–**4**, modeling data of all their located conformations, and comparison of the B3LYP/6-31G(d) and 6-311++G(2d,p) GIAO calculated ^{1}H NMR chemical shifts are presented.

Acknowledgments

The Authors thank Professor Michael Kay (University of Utah, U.S.A.) for helpful discussions. They acknowledge the financial support from the Universities of Pavia and Milano (FAR and PUR grants, respectively). The study was also supported by Grant no. 201433 from the European Commission/Seventh Framework Programme (FP7/2007–2013) and Grant GCE no. 53030 and PP1008144 from the Bill and Melinda Gates Foundation to L. Lopalco.

[1] R. C. Gallo, L. Montagnier, *New Engl. J. Med.* **2003**, *349*, 2283–2285.
[2] WHO/UNAIDS, AIDS Epidemic Update **2009**.
[3] a) V. Briz, E. Poveda, V. Soriano, *J. Antimicrob. Chemother.* **2006**, *57*, 619–627; b) S. Rusconi, A. Scozzafava, A. Mastrolorenzo, C. T. Supuran, *Curr. Drug Targets Infect. Disord.* **2004**, *4*, 339–355; c) F. Shaheen, R. G. Collman, *Curr. Opin. Infect. Dis.* **2004**, *17*, 7–16; d) I. Markovic, *Curr. Pharm. Des.* **2006**, *12*, 1105–1119.
[4] T. Wang, Z. Zhang, O. B. Wallace, M. Deshpande, H. Fang, Z. Yang, L. M. Zadjura, D. L. Tweedie, S. Huang, F. Zhao, S. Ranadive, B. S. Robinson, Y. F. Gong, K. Ricarrdi, T. P. Spicer, C. Deminie, R. Rose, H. G. H. Wang, W. S. Blair, P. Y. Shi, P. F. Lin, R. J. Colonno, N. A. Meanwell, *J. Med. Chem.* **2003**, *46*, 4236–4239.
[5] a) P. F. Lin, W. Blair, T. Wang, T. Spicer, Q. Guo, N. Zhou, Y. F. Gong, H. G. H. Wang, R. Rose, G. Yamanaka, B. Robinson, C. B. Li, R. Fridell, C. Deminie, G. Demers, Z. Yang, L. Zadjura, N. Meanwell, R. A. Colonno, *Proc. Natl. Acad. Sci. USA* **2003**, *100*, 11013–11018; b) Q. Guo, H.-T. Ho, I. Dicker, L. Fan, N. Zhou, J. Friborg, T. Wang, B. V. McAuliffe, H. H. Wang, R. E. Rose, H. Fang, H. T. Scarnati, D. R. Langley, N. A. Meanwell, R. Abraham, R. J. Colonno, P. F. Lin, *J. Virol.* **2003**, *77*, 10528–10536.
[6] R. S. Veazey, P. J. Klasse, S. M. Schader, Q. Hu, T. J. Ketas, M. Lu, P. A. Marx, J. Dufour, R. J. Colonno, R. J. Shattock, M. S. Springer, J. P. Moore, *Nature* **2005**, *438*, 99–102.
[7] D. Colombo, S. Villa, L. Solano, L. Legnani, F. Marinone Albini, L. Toma, *Eur. J. Org. Chem.* **2009**, 3178–3183.
[8] a) R.-J. Lu, J. A. Tucker, T. Zinevitch, O. Kirichenko, V. Konoplev, S. Kuznetsova, S. Sviridov, J. Pickens, S. Tandel, E. Brahmachary, Y. Yang, J. Wang, S. Freel, S. Fisher, A. Sullivan, J. Zhou, S. Stanfield-Oakley, M. Greenberg, D. Bolognesi, B. Bray, B. Koszalka, P. Jeffs, A. Khasanov, Y.-A. Ma, C. Jeffries, C. Liu, T. Proskurina, T. Zhu, A. Chucholowski, R. Li, C. Sexton, *J. Med. Chem.* **2007**, *50*, 6535–6544; b) T. Wang, Z. Yin, Z. Zhang, J. A. Bender, Z. Yang, G. Johnson, Z. Yang, L. M. Zadjura, C. J. D′Arienzo, D. DiGiugno Parker, C. Gesenberg, G. A. Yamanaka, Y.-F. Gong, H.-T. Ho, H. Fang, N. Zhou, B. V. McAuliffe, B. J. Eggers, L. Fan, B. Nowicka-Sans, I. B. Dicker, Q. Gao, R. J. Colonno, P.-F. Lin, N. A. Meanwell, J. F. Kadow, *J. Med. Chem.* **2009**, *52*, 7778–7787.
[9] M. Li, F. Gao, J. R. Mascola, L. Stamatatos, V. R. Polonis, M. Koutsoukos, G. Voss, P. Goepfert, P. Gilbert, K. M. Greene, M. Bilska, D. L. Kothe, J. F. Salazar-Gonzalez, X. Wei, J. M. Decker, B. H. Hahn, D. C. Montefiori, *J. Virol.* **2005**, *79*, 10108–10125.
[10] a) G. Loriga, I. Manca, G. Murineddu, G. Chelucci, S. Villa, S. Gessi, L. Toma, G. Cignarella, G. A. Pinna, *Bioorg. Med. Chem.* **2006**, *14*, 676–691; b) D. Barlocco, G. Cignarella, D. Tondi, P. Vianello, S. Villa, A. Bartolini, C. Gheraldini, N. Galeotti, D. J. Anderson, T. A. Kuntzweiler, D. Colombo, L. Toma, *J. Med. Chem.* **1998**, *41*, 674–681; c) G. A. Pinna, G. Murineddu, M. M. Curzu, S. Villa, P. Vianello, P. A. Borea, S. Gessi, L. Toma, D. Colombo, G. Cignarella, *Farmaco* **2000**, *55*, 553–562.
[11] N. Soundararajan, S. Benoit, S. Gingras (Squibb Bristol Myers Co.), PCT WO 03082289, **2003** [*Chem. Abstr.* **2003**, *139*, 307795].
[12] a) A. D. Becke, *J. Chem. Phys.* **1993**, *98*, 5648–5652; b) C. Lee, W. Yang, R. G. Parr, *Phys. Rev. B* **1988**, *37*, 785.
[13] a) V. Barone, M. Cossi, J. Tomasi, *J. Comput. Chem.* **1998**, *19*, 404–417; b) J. Tomasi, B. Mennucci, R. Cammi, *Chem. Rev.* **2005**, *105*, 2999–3093.
[14] a) K. Wolinski, F. James, J. F. Hinton, P. Pulay, *J. Am. Chem. Soc.* **1990**, *112*, 8251–8260; b) R. Ditchfield, *Mol. Phys.* **1974**, *27*, 789–807.
[15] GIAO NMR calculations were also performed by using the larger basis set 6-311++G(2d,p). However, a worsening of the errors was observed (see Supporting Information).
[16] M. J. Frisch, G. W. Trucks, H. B. Schlegel, G. E. Scuseria, M. A. Robb, J. R. Cheeseman, J. A. Montgomery Jr., T. Vreven, K. N. Kudin, J. C. Burant, J. M. Millam, S. S. Iyengar, J. Tomasi, V. Barone, B. Mennucci, M. Cossi, G. Scalmani, N. Rega, G. A. Petersson, H. Nakatsuji, M. Hada, M. Ehara, K. Toyota, R. Fukuda, J. Hasegawa, M. Ishida, T. Nakajima, Y.

Honda, O. Kitao, H. Nakai, M. Klene, X. Li, J. E. Knox, H. P. Hratchian, J. B. Cross, C. Adamo, J. Jaramillo, R. Gomperts, R. E. Stratmann, O. Yazyev, A. J. Austin, R. Cammi, C. Pomelli, J. W. Ochterski, P. Y. Ayala, K. Morokuma, G. A. Voth, P. Salvador, J. J. Dannenberg, V. G. Zakrzewski, S. Dapprich, A. D. Daniels, M. C. Strain, O. Farkas, D. K. Malick, A. D. Rabuck, K. Raghavachari, J. B. Foresman, J. V. Ortiz, Q. Cui, A. G. Baboul, S. Clifford, J. Cioslowski, B. B. Stefanov, G. Liu, A. Liashenko, P. Piskorz, I. Komaromi, R. L. Martin, D. J. Fox, T. Keith, M. A. Al-Laham, C. Y. Peng, A. Nanayakkara, M. Challacombe, P. M. W. Gill, B. Johnson, W. Chen, M. W. Wong, C. Gonzalez, J. A. Pople, *Gaussian 03, Revision B.04*, Gaussian, Inc., Pittsburgh, PA, **2003**.

Received: July 29, 2010
Published Online: November 22, 2010

